

Retraction

Retracted: Featureless Blood Pressure Estimation Based on Photoplethysmography Signal Using CNN and BiLSTM for IoT Devices

Wireless Communications and Mobile Computing

Received 10 October 2023; Accepted 10 October 2023; Published 11 October 2023

Copyright © 2023 Wireless Communications and Mobile Computing. This is an open access article distributed under the Creative Commons Attribution License, which permits unrestricted use, distribution, and reproduction in any medium, provided the original work is properly cited.

This article has been retracted by Hindawi following an investigation undertaken by the publisher [1]. This investigation has uncovered evidence of one or more of the following indicators of systematic manipulation of the publication process:

- (1) Discrepancies in scope
- (2) Discrepancies in the description of the research reported
- (3) Discrepancies between the availability of data and the research described
- (4) Inappropriate citations
- (5) Incoherent, meaningless and/or irrelevant content included in the article
- (6) Peer-review manipulation

The presence of these indicators undermines our confidence in the integrity of the article's content and we cannot, therefore, vouch for its reliability. Please note that this notice is intended solely to alert readers that the content of this article is unreliable. We have not investigated whether authors were aware of or involved in the systematic manipulation of the publication process.

Wiley and Hindawi regrets that the usual quality checks did not identify these issues before publication and have since put additional measures in place to safeguard research integrity.

We wish to credit our own Research Integrity and Research Publishing teams and anonymous and named external researchers and research integrity experts for contributing to this investigation.

The corresponding author, as the representative of all authors, has been given the opportunity to register their agreement or disagreement to this retraction. We have kept a record of any response received.

References

- [1] Y. Li, L. N. Harfiya, and C. Chang, "Featureless Blood Pressure Estimation Based on Photoplethysmography Signal Using CNN and BiLSTM for IoT Devices," *Wireless Communications and Mobile Computing*, vol. 2021, Article ID 9085100, 10 pages, 2021.

Research Article

Featureless Blood Pressure Estimation Based on Photoplethysmography Signal Using CNN and BiLSTM for IoT Devices

Yung-Hui Li ¹, Latifa Nabila Harfiya ², and Ching-Chun Chang ³

¹AI Research Center, Hon Hai Research Institute, Taipei 114699, Taiwan

²Department of Computer Science and Information Engineering, National Central University, Taoyuan 32001, Taiwan

³Department of Computer Science, University of Warwick, Coventry CV47AL, UK

Correspondence should be addressed to Latifa Nabila Harfiya; latifanaharfiya@gmail.com

Received 8 October 2021; Accepted 8 November 2021; Published 26 November 2021

Academic Editor: Chi-Hua Chen

Copyright © 2021 Yung-Hui Li et al. This is an open access article distributed under the Creative Commons Attribution License, which permits unrestricted use, distribution, and reproduction in any medium, provided the original work is properly cited.

Continuous blood pressure (BP) acquisition is critical to health monitoring of an individual. Photoplethysmography (PPG) is one of the most popular technologies in the last decade used for measuring blood pressure noninvasively. Several approaches have been carried out in various ways to utilize features extracted from PPG. In this study, we develop a continuous systolic and diastolic blood pressure (SBP and DBP) estimation mechanism without the need for any feature engineering. The raw PPG signal only got preprocessed before being fed to our model which mainly consists of one-dimensional convolutional neural network (CNN) and bidirectional long short-term memory (BiLSTM) network. We evaluate the resulting SBP and DBP value by the root-mean-squared error (RMSE) and mean absolute error (MAE). This study addresses the effectiveness of the model by outperforming the previous feature engineering-based methods. We achieve RMSE of 11.503 and 6.525 for SBP and DBP, respectively, and MAE of 7.849 and 4.418 for SBP and DBP, respectively. The proposed method is expected to substantially enhance the current efficiency of healthcare IoT (Internet of Things) devices in BP monitoring using PPG signals only.

1. Introduction

Blood pressure (BP) is a biomarker that interprets how much tension the blood exerts on a blood vessel wall for every unit area. The more tension the blood imposes on the blood vessel, the higher the BP value is. The measurement of BP occurs in the arterial blood vessels adjacent to the heart. This measurement is a direct function of ventricular contractions. BP can be measured as a function of the resistance through the blood vessels and blood flow [1]. Thus, BP dynamically fluctuates in response to the changes in diameter of the blood vessel, vessel length, and the viscosity of the blood. Hence, as the blood volume in the vessels becomes greater, so does the BP. All these changes are the consequences of a perplexing interchange between the environmental, physical, and emotional factors. Accordingly, BP might vary depending on the daily, hourly, or even minutely challenges of each individual [2].

The temporal dimensions and patterns characterizing the BP variations define the term BP variability (BPV). From a clinical perspective, BPV could be seen as a source of noise that creates difficulties in assessing the individual's "true" BP value. Evidence is now available to support its role also as an independent predictor of cardiovascular risk. While the BPV increases, the possibility of pharmacological treatment's target becomes higher as well [2]. On that account, monitoring continuous BP is critical in order to capture the absolute BP value of an individual.

Currently, there is one machine that can do accurate continuous measurement called Finapres [3] which uses a noninvasive method based on a photoplethysmographic system. The growth of Internet of Things (IoT) and wearable devices applied in healthcare industry makes it much easier to measure physiological signal in a noninvasive fashion, and it is undoubtedly good news for most patients. As they can do routine self-health monitoring, it helps them to get

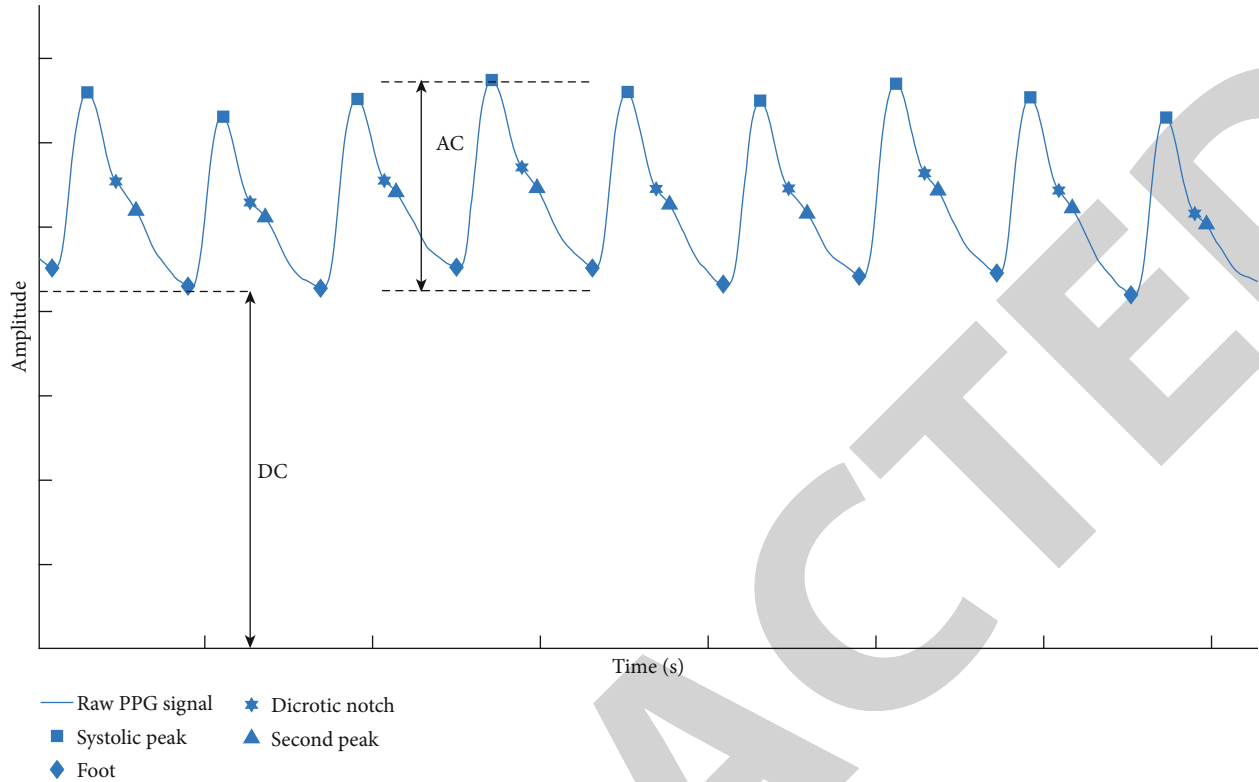


FIGURE 1: PPG signal's decomposition.

early warning about any abnormality for their health. In the last decade, numerous IoT-enabled wearable biosensor devices utilize Photoplethysmography (PPG) for monitoring the physiological conditions of a patient. In addition to the massive application in personal wearable IoT devices, PPG is also commonly applied in pulse oximetry due to its convenience and capacity to perform continuous readings [4]. Nevertheless, a PPG waveform discloses the cardiovascular and respiratory systems' activity of a patient in the corresponding time period [5].

A PPG waveform is designated with a pulsatile physiological waveform "AC." For every heartbeat, the cardiac synchronous alteration over the blood volume is reflected by this waveform. This waveform lays over a slowly varying baseline "DC" which contains lower frequency components. This part reflects the potential conditions related to respiration, thermoregulation, and skin tissue condition [6]. Blood is pumped by the heart to the periphery in each cardiac cycle. Amid the pressure that reaches the skin, arteries and arterioles are amplified in the subcutaneous tissue. The pressure pulse can be seen from the venous plexus upon a light reflex or disseminate detector device adhered to the skin as a secondary peak. On the other hand, the larger peak appears for each cardiac cycle which the blood volume alters due to the pressure pulse captured by illuminating the skin with a Light-Emitting Diode (LED) and photodetector, namely, photodiode, which measures how much is the transmitted or reflected light [7], as seen in Figure 1.

In Figure 1, parameters that are commonly utilized to generate features in PPG for BP estimation [7–13] are pre-

sented such as systolic peak, foot, dicrotic notch, and the second peak. Various approaches, namely, pulse transit time (PTT), pulse arrival time (PAT), and pulse wave velocity (PWV), are extracted using given parameters from two PPG sensors located on two distant sites. These parameters, however, may not always appear in the signal mostly due to the moving artifacts in the process of acquisition [14]. Automatic feature extraction from PPG signal is becoming a necessity since noises are hard to handle even with complex feature engineering [15]. Prior studies [13, 16] have successfully predicted BP using complex time series modelling such as long short-term memory (LSTM) network with a low error. These methods, however, tried to skip every defined range of signal with unhandled noise which is discontinuous in nature.

Herein, the purpose of this study is twofold. First, we develop a continuous BP estimation framework without plethoric concern about how to extract features. As the use of IoT devices for healthcare purposes provides benefits for people to monitor themselves, applying featureless framework for inferencing is expected to reliably lessen the response time and the computing cost. Second, we propose a robust deep learning model to do the automatic feature extraction as well as the BP estimation. Convolutional neural network (CNN) has been shown to be the state-of-the-art when it comes to automatic feature extraction while LSTM is an effective choice for analyzing time series data with an ability to handle long sequential data. PPG signal is obviously a one-dimensional signal which varies with time. This study, hence, will utilize the 1D CNN and bidirectional

LSTM (BiLSTM) network to train a deep learning model for the BP estimation. The output will be the estimated values of two types of BP, which are systolic blood pressure (SBP) and diastolic blood pressure (DBP). Related works using different methods are described in Section 2. We provide the detail of our proposed model in Section 3. We then present the result of the model's evaluation in Section 4 followed by the comparative analysis of the foregoing result and conclude it in Section 5.

2. Related Works

2.1. Feature-Based BP Estimation. BP is known to have a nonlinear relationship with PTT which is commonly obtained by measuring the time difference between the electrocardiogram (ECG) R peak and the maximum slope of the corresponding PPG signal [16]. Aside from PTT, various features extracted from PPG are found to be correlated with BP. The amplitude of systolic shown in Figure 1 indicates the pulsatile transformation in blood volume due to the arterial blood flow alongside the distal site. Moreover, the systolic amplitude is prompt to be a more appropriate parameter for BP estimation instead of PTT [17]. A number of features from PPG which have been proposed in [12, 14] are listed as follows (see Figure 2(a)):

- (i) Augmentation index (AI) which equals to y/x
- (ii) Large Artery Stiffness Index (LASI) or S_3
- (iii) Inflection Point Area ratio (IPA), denoted by S_1 , S_2 , S_3 , and S_4
- (iv) Cardiac period (CP)
- (v) Systolic upstroke time (SUT)
- (vi) Diastolic time (DT)
- (vii) Systolic width (SW) at a % of maximum amplitude
- (viii) Diastolic width (DW) at a % of maximum amplitude

The inference process is performed using regression-based supervised machine learning algorithms including support vector machine (SVM) and artificial neural network (ANN). Additional investigation based on new-time domain features has been done in [18]. In the study, it is also found that Womersley number which interprets the influence of fluid flow properties on BP affects the accuracy. The best prediction result is done using random forest (RF) with a genetic algorithm (GA) as the feature selection method for minimizing the computational cost. Deeper investigation to the PPG signal's derivatives not only alleviates the number of features but also reduces the estimation errors in our previous work [19]. From the original PPG signal, the first derivative (dPPG) and the second derivative (sdPPG) are computed to generate new parameters, i.e., the ascending and descending area of dPPG defined as dAA and dDA, respectively, and the ascending and descending area of sdPPG defined as sdAA and sdDA, respectively, as shown in Figure 2. In this work, a four-layered deep neural network

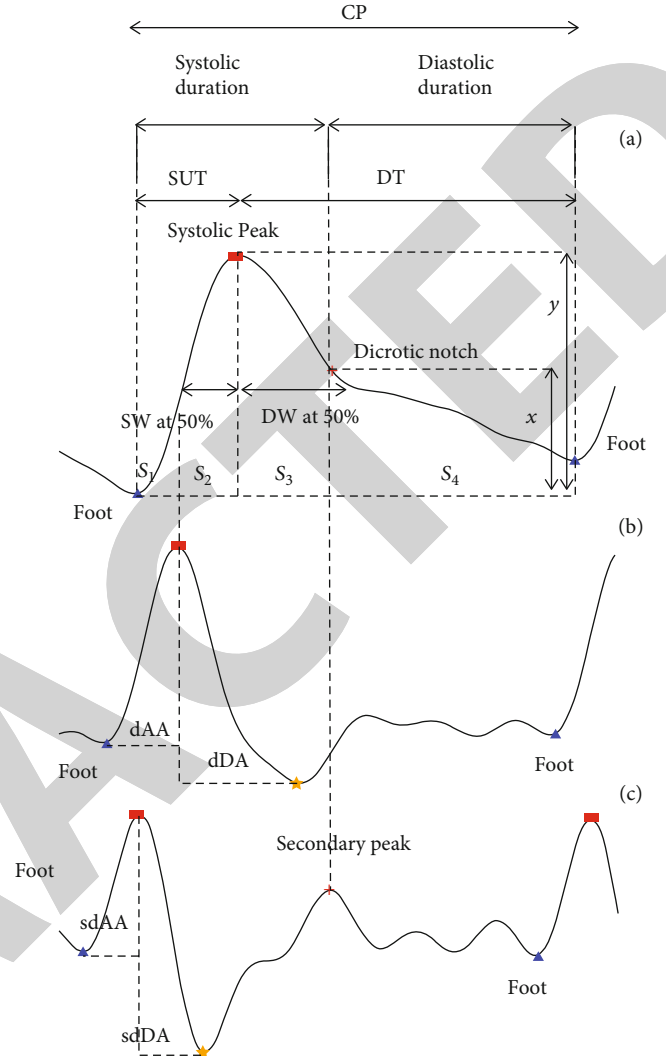


FIGURE 2: (a) PPG, (b) dPPG, and (c) sdPPG.

is suggested as the best algorithm to predict SBP and DBP from the input of 59 features. However, the size of the network is quite large which requires high computing resource.

2.2. Featureless-Based BP Estimation. The PPG waveform varies over subjects due to various influences such as age, drugs, and diseases. There are four typical waveform variations of PPG waveform [15], as shown in Figure 3. The ideal waveform is mostly found from cardiovascular disease-free people illustrated in Figure 3(a). Figures 3(b) and 3(c) show waveform with an indistinct and almost nonexistent dicotic notch while Figure 3(d) shows an invisible dicotic notch with diastolic duration that decays faster than the others. Thus, extracting handcraft features from nonideal waveform will be difficult to carry out in practice and automatic extraction of necessary features is proposed.

In [15], automatic extraction is performed using ANN with the input consisting of ECG and PPG signals. The output features are fed to a three-layered LSTM network to learn the generated features and predict the SBP and DBP. Instead of using multiple sensors for the data acquisition,

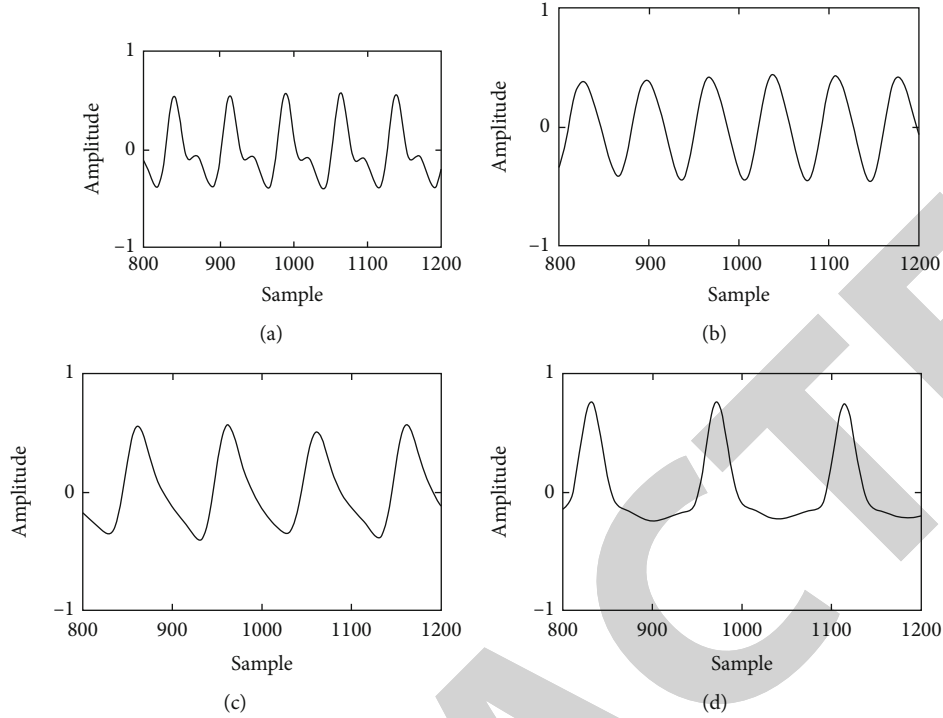


FIGURE 3: Waveform variations of PPG waveform including (a) ideal, (b), (c), and (d) nonideal [14].

automatic extraction from PPG signal only has been verified by [20] using a CNN which consists of an input layer, a convolutional layer, a pooling layer, and two fully connected layers. Using the PPG and its first and second derivatives, the estimation result is reported to be improved compared to the traditional method (i.e., applying multiple regression analysis of the pulse wave). However, large errors can still be found for the cases of extremely high or low SBP.

3. Materials and Methods

In this study, a new approach to estimate continuous blood pressure from PPG signal without feature engineering is proposed. Specifically, the data and structured steps to embody the proposed methodology are explained in this section.

3.1. Dataset. The PPG signal is obtained from Multiparameter Intelligent Monitoring in Intensive Care (MIMIC) II database [12, 21] which contains PPG records from more than 10,000 subjects with normal and abnormal cases. This dataset provides arterial blood pressure (ABP) signal from the related subjects as well. We extract the SBP and DBP values from the corresponding ABP signals and use them for the ground truth in the process of training and testing.

3.2. Preprocessing

3.2.1. Segmentation. Before signals are being trained with our model, signal segmentation is carried out. We define one segment of signal that begins at one PPG's foot to the following foot consecutively. Thus, we conduct a foot detection anterior to the segmentation.

3.2.2. Resampling. PPG signals are recorded from subjects with varying conditions. The waveforms exhibit varying frequency and the length of the PPG with different subjects. For signal length normalization, we avoid zero padding considering that the padded signal might contain zeros up to 50% of the final length which impacts the model negatively. Instead, we applied signal interpolation. Thus, each of the PPG segments is resampled to 700 data points in order to unify the length of all segments.

3.3. Partitioning. After performing preprocessing on the dataset, we obtain more than 100,000 resampled PPG segments. We then randomly select 50,165 segments and partitioned them into three sets. The first set is the training set which is 80% of the total selected data. The second set is the validation set which is 10% of the training set. Lastly, the third set is the testing set which is the rest 20% of the total selected data. Given that partitioning, we are certain that our model is trained and tested using completely disjointed data.

3.4. Evaluation Metrics. The root-mean-squared error (RMSE), mean absolute error (MAE), and also standard deviation (STD) of estimation error are used for the model evaluation on the disjointed test set. We also present an evaluation based on the Association for the Advancement of the Medical Instrumentation (AAMI) standard [22] and British Hypertension Society (BHS) standard [23].

3.5. Overall Estimator Network

3.5.1. CNN. The success of CNN in many tasks related to image segmentation, classification, retrieval, and also

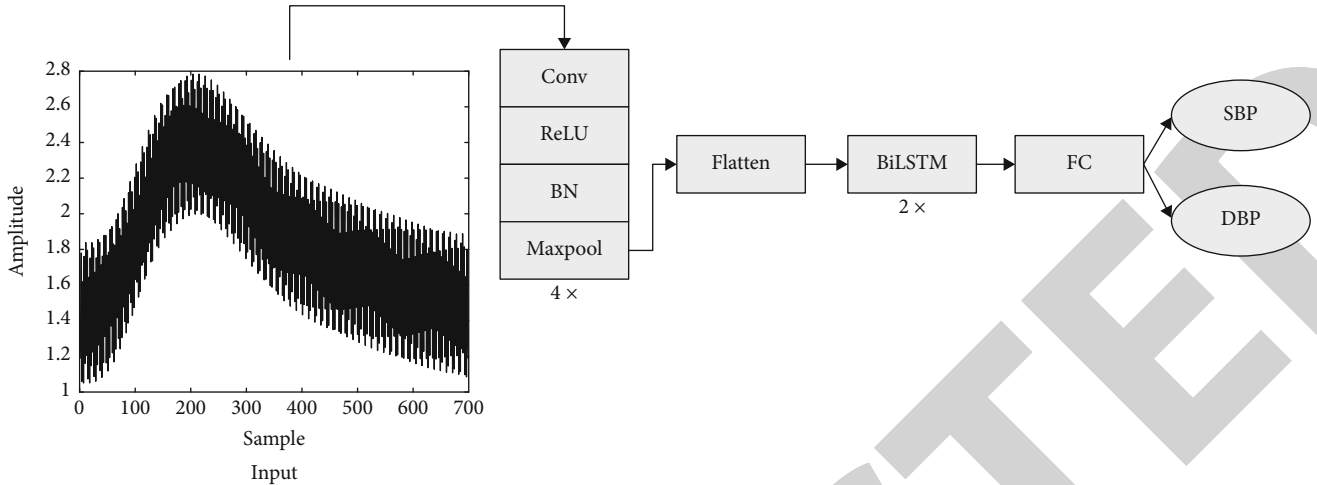


FIGURE 4: Illustration of the proposed network model.

captioning [24, 25] is because of its ability to exploit either the spatial or temporal correlation within the data [26–28]. In general, a typical CNN architecture includes convolution and pooling layer which is followed by a fully connected layer as the last layer. The convolutional layer works through slicing the input into small slices, commonly acknowledged as receptive fields. By slicing it into small pieces, the network is encouraged to understand feature motifs. The feature motifs may occur at various locations. However, the precise location becomes less relevant once important features are extracted, as long as its approximate position relative to others is retained. The pooling operation facilitates the network to extract a combination of features by summing up similar information in the neighbourhood. Thus, its components are making CNN a great option for automatic feature extractor.

3.5.2. BiLSTM. The memory cell that can maintain its state over time and its nonlinear gating units that thoroughly control the information flow is the key point behind the LSTM’s success in resolving the long sequence problem [26]. While BiLSTM tries to connect two hidden layers of LSTM (i.e., the input sequence and the reverse copy of the corresponding sequence), it enhances the ability to learn longer dependency and subsequently improve the model performance. There are four modes how the BiLSTM connects the hidden layers, such as the following:

- (i) Concat: concatenating the output of both layers
- (ii) Mul: multiplying the output of both layers
- (iii) Sum: adding the output of both layers
- (iv) Ave: taking the average of both layers’ output

Assume that having an input sequence with the size of $n \times t \times c$, which denotes number of batch size, number of timesteps, and number of states, respectively, the “mul,” “sum,” and “ave” mode will return an output size of $n \times t \times c$. Otherwise, the “concat” mode will return an output size of $n \times t \times 2c$ which is more informative since it does not lose

any information from both input sequence (forward) and its reverse copy (backward). In this way, it allows the model to learn where to pick information and generates lower loss in the training process. Given that BiLSTM comprises of a forward LSTM and a backward LSTM layer, it performs better prediction significantly [29, 30]. The success of BiLSTM is also proved in BP estimation task, reported in [16]. Therefore, we adopt BiLSTM architecture in our BP estimation model.

Accordingly, the proposed network is a model consisting of two hierarchy levels. The lower hierarchy level uses CNN layers to extract necessary features. The upper level uses BiLSTM to do the estimation by learning the temporal relations among the features extracted in the lower hierarchy. Each of the resampled PPG segments is the input into the CNN layers. The output of CNN layers then will be fed up to the BiLSTM layers which then output a regression result of SBP and DBP. The general illustration is shown in Figure 4.

The proposed model comprises of four 1D CNN layers which are followed by rectified linear unit (ReLU) activation function, batch normalization (BN), and max pooling in each layer. The output from the last max-pooling layer is then being flatten to be the input for two BiLSTM layers with “concat” mode. The last layer of the proposed model is a fully connected (FC) layer which generates regression output of SBP and DBP value. This model is trained using MATLAB 2019B with one GPU (NVIDIA GeForce GTX 750 Ti) within 20 epochs. We set the batch size into 128 and the initial learning rate is 0.001 which is then decreased by a factor of 0.1 every 175 iterations. The detailed information about the proposed model along with the best hyperparameter setting is presented in Table 1.

4. Results and Discussion

The testing results from our proposed model are presented in Table 2. In the first four rows of Table 2, we compare our result with previous studies which are based on feature engineering method in terms of RMSE, MAE, and STD of

TABLE 1: Network architecture.

Layer	Filter size	#filter/hidden units	Input size
Input	—	—	$1 \times 700 \times 1$
Conv_1	1×350	2	$1 \times 700 \times 2$
ReLU_1	—	—	$1 \times 700 \times 2$
BN_1	—	—	$1 \times 700 \times 2$
Maxpool_1	1×175	—	$1 \times 700 \times 2$
Conv_2	1×175	10	$1 \times 700 \times 10$
ReLU_2	—	—	$1 \times 700 \times 10$
BN_2	—	—	$1 \times 700 \times 10$
Maxpool_2	1×25	—	$1 \times 700 \times 10$
Conv_3	1×25	20	$1 \times 700 \times 20$
ReLU_3	—	—	$1 \times 700 \times 20$
BN_3	—	—	$1 \times 700 \times 20$
Maxpool_3	1×10	—	$1 \times 700 \times 20$
Conv_4	1×10	40	$1 \times 700 \times 40$
ReLU_4	—	—	$1 \times 700 \times 40$
BN_4	—	—	$1 \times 700 \times 40$
Maxpool_4	1×5	—	$1 \times 700 \times 40$
Flatten	—	—	28000
BiLSTM_1	—	128	256
BiLSTM_2	—	350	700
FC	—	—	2

TABLE 2: Performance of different approaches.

Model	Input	SBP (mmHg)			DBP (mmHg)		
		RMSE	MAE	STD	RMSE	MAE	STD
SVM [12]	5 features from ECG & PPG	—	12.38	16.17	—	6.34	8.45
SVR [31]	35 features from PPG	10.9	8.54	—	5.8	4.34	—
NN [31]	35 features from PPG	11.6	13.4	—	5.9	6.9	—
RF [18]	>15 features from ECG & PPG	13.83	9.54	—	6.80	5.48	—
1DCNN + LSTM	Raw PPG signal	13.49	8.92	8.23	8.78	6.14	5.22
Proposed	Raw PPG signal	11.50	7.85	8.41	6.53	4.42	4.80

the estimation results. The first work [12] uses the MIMIC II dataset and uses 4,254 records for the experiments. Each record contains predefined features extracted from PPG and ECG signal such as pulse transit time (PTT) and heart rate (HR). The study uses regularized linear regression (RLR), artificial neural network (ANN), and support vector machine (SVM) approaches to do the prediction.

Here, we compare our result with the result from the SVM approach which is the best one. The second and third studies are from [31] which used merely 910 good PPG signals from the MIMIC II dataset. The study uses 35 features extracted from the obtained PPG to train a neural network (NN) and support vector regression (SVR) as the estimator. Given that the results are acceptable, we compare our result

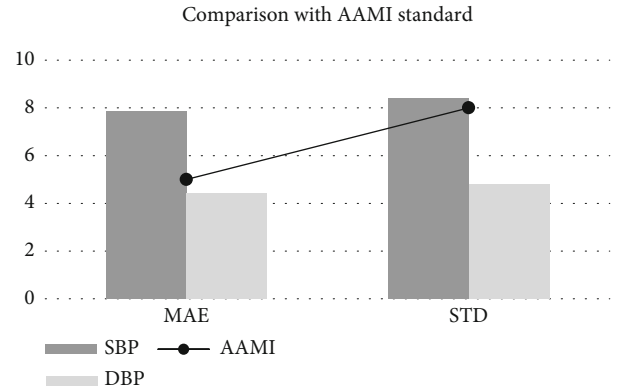


FIGURE 5: Comparison with AAMI standard.

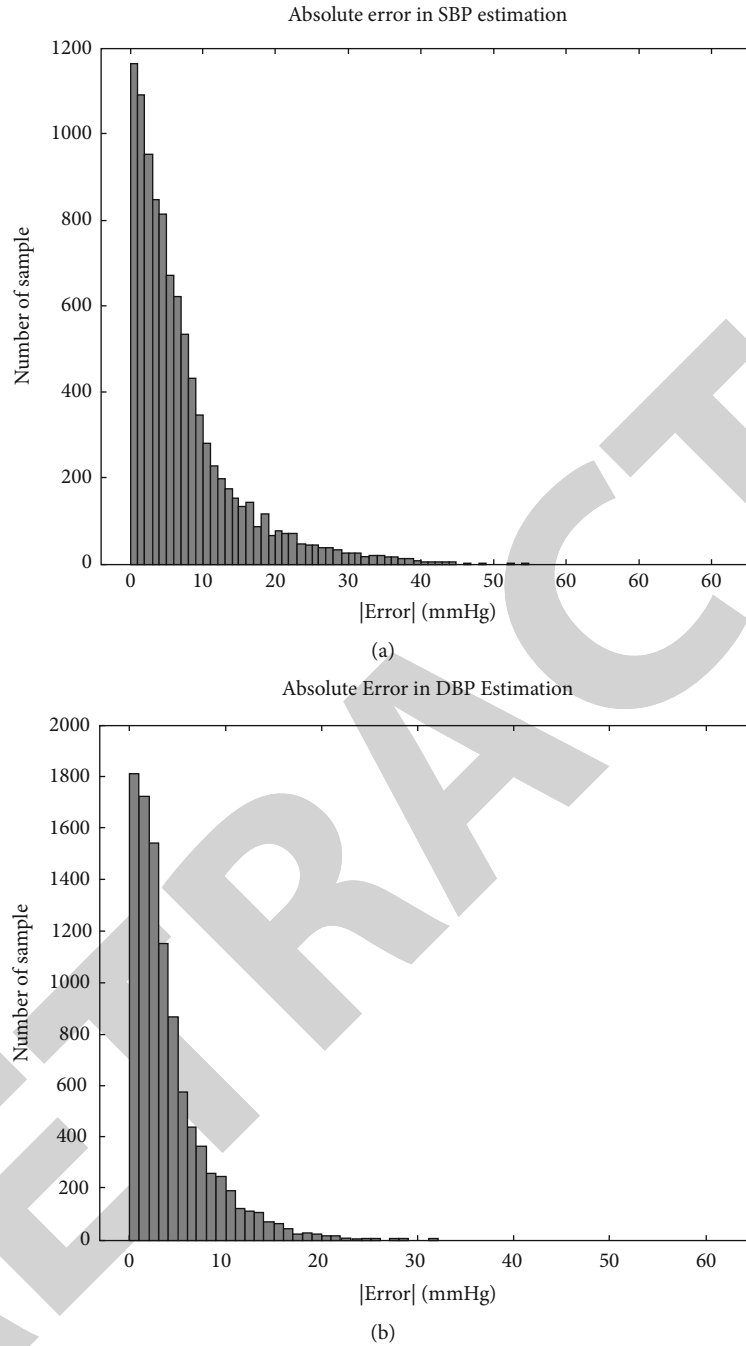


FIGURE 6: Histogram of absolute error in (a) SBP estimation and (b) DBP estimation.

to both of them. The results shown in the fourth row are depicted from [18] which utilized 43 features from ECG and PPG signal obtained from the MIMIC II dataset. To minimize estimation error, the genetic algorithm is used to discard negligible features. Several machine learning approaches are used as a predictor in this study, and random forest (RF) was reported as the most accurate predictor among them. To verify the benefit of BiLSTM in the network, we build a twin network that uses unidirectional LSTM instead of BiLSTM. With the same number of layers, hidden nodes, and settings, we can see how BiLSTM can affect the model performance.

The AAMI standard requires both SBP and DBP estimators to have mean error and standard deviation error below 5 and 8 mmHg, respectively, measured on a dataset consisting of more than 85 subjects. In our case, only the DBP estimator satisfies the AAMI standard while the SBP estimator slightly missed with the STD restriction as shown in Figure 5. Figure 6 presents the distribution of the absolute error of SBP and DBP estimation, respectively. The comparison result with the BHS standard concludes that our SBP estimator reaches grade C while our DBP estimator exceeds the standard with grade A which can be seen in Figure 7 with the criterion specifically presented in Table 3.

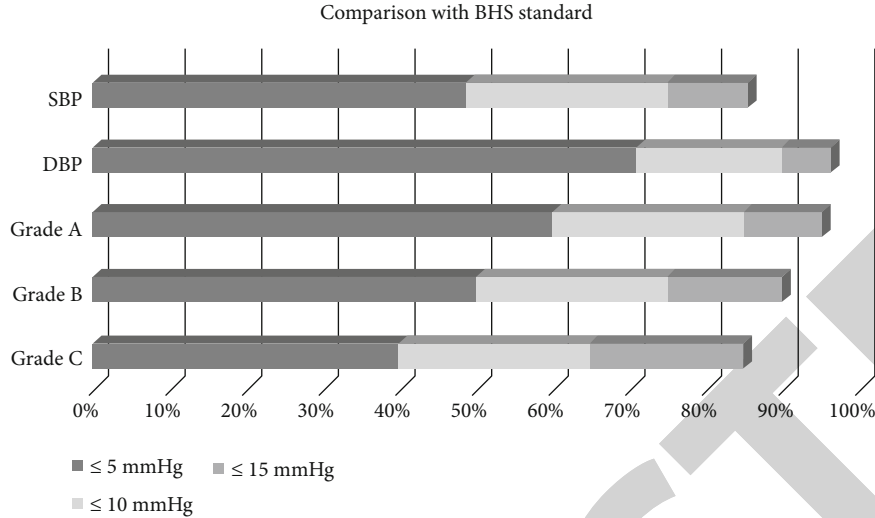


FIGURE 7: Comparison with BHS standard.

TABLE 3: Comparison with BHS standard.

Cumulative error		≤5 mmHg	≤10 mmHg	≤15 mmHg
Our result	SBP	48.69%	74.92%	85.49%
	DBP	70.84%	89.98%	96.38%
	Grade A	60%	85%	95%
BHS	Grade B	50%	75%	90%
	Grade C	40%	65%	85%

4.1. Comparison with Prior Studies. It is doubtless that conducting a fair comparison with prior studies is difficult due to the following reasons. Although all the studies being compared use the MIMIC II dataset, the number of subjects being used in each study are varying. Moreover, the evaluation metrics presented in every study are also different which cannot portray a comprehensive comparison. Nevertheless, we tried our best to summarize the existing work and compared the proposed method with them. Table 2 compares the performance of various existing methods with the proposed method, in terms of RMSE, MAE, and STD. We can see that the proposed method outperforms other methods except for SVR [31]. However, the method in [31] needs to select 35 features by the domain expert, while with the proposed method, we can directly feed the raw PPG signal into the system and get the result. The number of records that are used in this study is more than 50,000 segments, which are also chosen randomly from 100,000 segments by doing segmentation on signals of 5000 subjects, which is much larger than in [31] (910 records of good signal). Thus, we speculate that there may be high variance in the data. In this case, the higher error can be addressed due to this problem. It is also evident that using bidirectional LSTM can reduce the estimation error. Both SBP and DBP predictions are significantly improved with BiLSTM compared to 1D CNN + LSTM. We confirm that learning the information extracted from the convolution layer not only in a forward manner but also in a backward manner can help the framework to understand its pattern better.

4.2. Perspective. The method in [31] which achieves the least error in the comparison experiment can be treated as an approach of classic “feature-based” signal processing while the proposed method is an “end-to-end” machine learning technique which can be treated as “featureless” signal processing. It does not require prior knowledge about the specific domain and therefore saves a lot of extra costs and is more preferred in the deep learning community. Using a deep learning method with a featureless processing can also save time [32] which will be very practical to be applied at wearable devices. Although we focus on PPG signals only in this study, this “featureless” signal processing can be a starting point for the other application using one-dimensional signal such as ECG, BCG, etc. We believe that in the future, “end-to-end” training, which needs no prior domain knowledge in the loop, will become more popular as the amount of data and computational resources increases. The transition from “feature-based” to “featureless” signal processing will be a paradigm shift in the domain of biomedical signal processing.

5. Conclusions

Despite the fact that the PPG sensor is becoming very popular for measuring SBP and DBP noninvasively, PPG signal can be easily affected by noise, especially during the signal acquisition stage. The challenge of extracting feature from poor quality of PPG signals for doing the measurement has been concluded by our model which discards feature engineering process by applying 1D CNN and BiLSTM network. Our model achieved acceptable SBP and DBP estimation results in terms of RMSE, MAE, and STD of the estimation error. It also satisfies the AAMI standard on DBP estimation and achieves grade C and grade A for SBP and DBP estimation, respectively. Through its simplicity and sufficiency, the proposed model can be applied into healthcare IoT devices. Moreover, further investigation on the model optimization such as applying an attention mechanism is required to improve the model’s performance and reduce the resulting error.

Data Availability

The MIMIC II dataset used to support the findings of this study have been deposited in the UCI Machine Learning repository (<https://archive.ics.uci.edu/ml/datasets/Cuff-Less+Blood+Pressure+Estimation>)

Conflicts of Interest

The authors declare that there is no conflict of interest regarding the publication of this paper.

References

- [1] H. Peterson, "Factors affecting blood pressure," *Access*, 2020, http://www.indianhills.edu/_myhills/courses/BIO178/documents/lu04_bp.pdf.
- [2] G. Parati, G. S. Stergiou, E. Dolan, and G. Bilo, "Blood pressure variability: clinical relevance and application," *The Journal of Clinical Hypertension*, vol. 20, no. 7, pp. 1133–1137, 2018.
- [3] P. Andriessen, R. L. M. Schoffelen, R. C. M. Berendsen et al., "Noninvasive assessment of blood pressure variability in pre-term infants," *Pediatric Research*, vol. 55, no. 2, pp. 220–223, 2004.
- [4] C. El-Hajj and P. A. Kyriacou, "A review of machine learning techniques in photoplethysmography for the non-invasive cuff-less measurement of blood pressure," *Biomedical Signal Processing and Control*, vol. 58, article 101870, 2020.
- [5] J. L. Moraes, M. X. Rocha, G. G. Vasconcelos, J. E. Vasconcelos Filho, V. H. C. de Albuquerque, and A. R. Alexandria, "Advances in photoplethysmography signal analysis for biomedical applications," *Sensors*, vol. 18, no. 6, p. 1894, 2018.
- [6] J. Allen, "Photoplethysmography and its application in clinical physiological measurement," *Physiological Measurement*, vol. 28, no. 3, pp. R1–R39, 2007.
- [7] F. Rundo, A. Ortis, S. Battiato, and S. Conoci, "Advanced bio-inspired system for noninvasive cuff-less blood pressure estimation from physiological signal analysis," *Computation*, vol. 6, no. 3, p. 46, 2018.
- [8] S. Chen, Z. Ji, H. Wu, and Y. Xu, "A non-invasive continuous blood pressure estimation approach based on machine learning," *Sensors*, vol. 19, no. 11, p. 2585, 2019.
- [9] X. Ding, B. P. Yan, Y.-T. Zhang, J. Liu, N. Zhao, and H. K. Tsang, "Pulse transit time based continuous cuffless blood pressure estimation: a new extension and a comprehensive evaluation," *Scientific Reports*, vol. 7, no. 1, article 11554, 2017.
- [10] W. H. Lin, X. Li, Y. Li, G. Li, and F. Chen, "Investigating the physiological mechanisms of the photoplethysmogram features for blood pressure estimation," *Physiological Measurement*, vol. 41, no. 4, article 044003, 2020.
- [11] P. Su, X. Ding, Y. Zhang, J. Liu, F. Miao, and N. Zhao, "Long-term blood pressure prediction with deep recurrent neural networks," in *2018 IEEE EMBS International Conference on Biomedical & Health Informatics (BHI)*, pp. 323–328, Las Vegas, NV, USA, 2018.
- [12] M. Kachuee, M. M. Kiani, H. Mohammadzade, and M. Shabany, "Cuff-less high-accuracy calibration-free blood pressure estimation using pulse transit time," in *2015 IEEE International Symposium on Circuits and Systems (ISCAS)*, pp. 1006–1009, Lisbon, Portugal, 2015.
- [13] F. P. Lo, C. X. Li, J. Wang, J. Cheng, and M. Q. Meng, "Continuous systolic and diastolic blood pressure estimation utilizing long short-term memory network," in *2017 39th Annual International Conference of the IEEE Engineering in Medicine and Biology Society (EMBC)*, pp. 1853–1856, Jeju, Korea, 2017.
- [14] Y. Kurylyak, F. Lamonaca, and D. Grimaldi, "A neural network-based method for continuous blood pressure estimation from a PPG signal," in *2013 IEEE International Instrumentation and Measurement Technology Conference (I2MTC)*, pp. 280–283, Minneapolis, MN, USA, 2013.
- [15] M. S. Tanveer and M. K. Hasan, "Cuffless blood pressure estimation from electrocardiogram and photoplethysmogram using waveform based ANN-LSTM network," *Biomedical Signal Processing and Control*, vol. 51, pp. 382–392, 2019.
- [16] Y.-H. Li, L. N. Harfiya, K. Purwandari, and Y.-D. Lin, "Real-time cuffless continuous blood pressure estimation using deep learning model," *Sensors*, vol. 20, no. 19, p. 5606, 2020.
- [17] M. Elgendi, "On the analysis of fingertip photoplethysmogram signals," *Current Cardiology Reviews*, vol. 8, no. 1, pp. 14–25, 2012.
- [18] G. Thambiraj, U. Gandhi, U. Mangalanathan, V. J. M. Jose, and M. Anand, "Investigation on the effect of Womersley number, ECG and PPG features for cuff less blood pressure estimation using machine learning," *Biomedical Signal Processing and Control*, vol. 60, article 101942, 2020.
- [19] Y.-C. Hsu, Y.-H. Li, C.-C. Chang, and L. N. Harfiya, "Generalized deep neural network model for cuffless blood pressure estimation with photoplethysmogram signal only," *Sensors*, vol. 20, no. 19, p. 5668, 2020.
- [20] S. Shimazaki, H. Kawanaka, H. Ishikawa, K. Inoue, and K. Oguri, "Cuffless blood pressure estimation from only the waveform of photoplethysmography using CNN," in *2019 41st Annual International Conference of the IEEE Engineering in Medicine and Biology Society (EMBC)*, pp. 5042–5045, Berlin, Germany, 2019.
- [21] M. Saeed, M. Villarroel, A. T. Reisner et al., "Multiparameter intelligent monitoring in intensive care II: a public-access intensive care unit database," *Critical Care Medicine*, vol. 39, no. 5, pp. 952–960, 2011.
- [22] American National Standard Manual, *Electronic or Automated Sphygmonanometers*, AAMI, 2003.
- [23] E. O'Brien, J. Petrie, W. Littler et al., "The British Hypertension Society protocol for the evaluation of automated and semi-automated blood pressure measuring devices with special reference to ambulatory systems," *Journal of Hypertension*, vol. 8, no. 7, pp. 607–619, 1990.
- [24] K. He, G. Gkioxari, P. Dollár, and R. Girshick, "Mask r-cnn," in *Proceedings of the IEEE international conference on computer vision*, pp. 2961–2969, Venice, Italy, 2017.
- [25] F. Schroff, D. Kalenichenko, and J. Philbin, "Facenet: a unified embedding for face recognition and clustering," in *Proceedings of the IEEE conference on computer vision and pattern recognition*, pp. 815–823, Boston, USA, 2015.
- [26] A. Khan, A. Sohail, U. Zahoor, and A. S. Qureshi, "A survey of the recent architectures of deep convolutional neural networks," *Artificial Intelligence Review*, vol. 53, no. 8, pp. 5455–5516, 2020.
- [27] L. Lo, H.-X. Xie, H.-H. Shuai, and W.-H. Cheng, "Facial chirality: using self-face reflection to learn discriminative features for facial expression recognition," in *The 2021 IEEE*

- International Conference on Multimedia & Expo (ICME)*, pp. 1–6, Shenzhen, China, 2021.
- [28] H.-X. Xie, L. Lo, H.-H. Shuai, and W.-H. Cheng, “AU-assisted graph attention convolutional network for micro-expression recognition,” in *The 28th ACM International Conference on Multimedia (MM 2020)*, pp. 2871–2880, Seattle, USA, 2020.
- [29] A. Graves and J. Schmidhuber, “Framewise phoneme classification with bidirectional LSTM and other neural network architectures,” *Neural Networks*, vol. 18, no. 5-6, pp. 602–610, 2005.
- [30] S. Siami-Namini, N. Tavakoli, and A. S. Namin, “The performance of LSTM and BiLSTM in forecasting time series,” in *2019 IEEE International Conference on Big Data (Big Data)*, pp. 3285–3292, Los Angeles, CA, USA, 2019.
- [31] M. Liu, L. M. Po, and H. Fu, “Cuffless blood pressure estimation based on photoplethysmography signal and its second derivative,” *International Journal of Computer Theory and Engineering*, vol. 9, no. 3, pp. 202–206, 2017.
- [32] J. Sanchez-Riera, K.-L. Hua, Y.-S. Hsiao, T. Lim, S. C. Hidayati, and W.-H. Cheng, “A comparative study of data fusion for RGB-D based visual recognition,” *Pattern Recognition Letters*, vol. 73, pp. 1–6, 2016.